

# Facile Fabrication of Titanium Carbide (Ti<sub>3</sub>C<sub>2</sub>)-Bismuth Vanadate (BiVO<sub>4</sub>) Nano-Coupled Oxides for Anti-cancer Activity

Received 04/15/2024

Review began 05/13/2024

Review ended 05/24/2024

Published 06/01/2024

© Copyright 2024

Lakshmi Anvitha et al. This is an open access article distributed under the terms of the Creative Commons Attribution License CC-BY 4.0., which permits unrestricted use, distribution, and reproduction in any medium, provided the original author and source are credited.

Nagubandi Lakshmi Anvitha<sup>1</sup>, Geetha A<sup>1</sup>, Vasugi S<sup>1</sup>, Balachandran S<sup>1</sup>, Ilango I.G.K<sup>1</sup>

<sup>1</sup>. Department of Physiology, Saveetha Dental College and Hospitals, Saveetha Institute of Medical and Technical Sciences (SIMATS) Saveetha University, Chennai, IND

**Corresponding author:** Ilango I.G.K, ilangoivarigk.sdc@saveetha.com

## Abstract

### Background

MXene is a newly discovered substance consisting of 2D transition metal carbides or nitrides, produced through the disintegration and etching of aluminum layers. It possesses numerous properties, including a high surface area, conductivity, strength, stiffness, negative zeta potential, and excellent volumetric capacitance. MXene is utilized in detecting anti-cancer medicine, while bismuth vanadate (BiVO<sub>4</sub>) is synthesized to form an optimized material for anti-cancer activity applications. BiVO<sub>4</sub> exhibits visible light absorption, strong chemical stability, and non-toxic properties. However, when loaded onto target stem cells, it can cause skin and respiratory irritation.

### Aim

This study aimed to evaluate the facile fabrication of titanium carbide (Ti<sub>3</sub>C<sub>2</sub>)-BiVO<sub>4</sub> nanomaterials coupled with oxides for anti-cancer activity. Moreover, it aimed to create Ti<sub>3</sub>C<sub>2</sub>-BiVO<sub>4</sub> nanomaterials in combination with oxides using X-ray diffraction (XRD) and scanning electron microscopy (SEM) to assess their potential as efficient and targeted anti-cancer agents.

### Methods and materials

To prepare the 2D Ti<sub>3</sub>C<sub>2</sub> MXene, 2.5 g of titanium aluminum carbide (Ti<sub>3</sub>AlC<sub>2</sub>) powder was dissolved in 60 mL of a 40% hydrofluoric acid (HF) solution in a polytetrafluoroethylene (PTFE) container. The etching process was made more efficient and completed in 24 hours by using a magnetic stirring system to keep the mixture stirred and heated continuously. The centrifugation was performed at 4000 rpm for five minutes. Subsequently, deionized water was used to wash the solution many times until its pH reached around 7. The appropriate Ti<sub>3</sub>C<sub>2</sub> powder was made by vacuum drying the acquired sediment at 80°C for 24 hours.

Monoclinic BiVO<sub>4</sub> samples were synthesized via a hydrothermal method. Typically, 10 mmol of Bi(NO<sub>3</sub>)<sub>3</sub>·5H<sub>2</sub>O was dissolved in 100 mL of a 2 mol/L HNO<sub>3</sub> solution and stirred uniformly. Subsequently, 10 mmol of ammonium metavanadate (NH<sub>4</sub>VO<sub>3</sub>) was added to the mixed solution. After being stirred for one hour, the mixture was transferred into a 100 mL sealed Teflon-lined stainless steel autoclave at 180°C for 16 hours. After cooling to room temperature, the sediment was washed three times with deionized water, ethanol, and acetone, respectively. Finally, the suspension was dried at 80°C, followed by calcination at 450°C for three hours to obtain BiVO<sub>4</sub>. Ti<sub>3</sub>C<sub>2</sub>-BiVO<sub>4</sub> heterostructures were prepared by surface modification Ti<sub>3</sub>C<sub>2</sub> using BiVO<sub>4</sub> suspensions by a simple, cost-effective approach.

### Results

Ti<sub>3</sub>C<sub>2</sub> nanosheets were observed with BiVO<sub>4</sub> particles, and the high crystalline nature of the compound was confirmed after XRD analysis and energy-dispersive spectroscopy (EDS) analysis. The compound was found to be pure without any impurities and exhibited anti-cancer activity.

### Conclusion

The XRD, field emission scanning electron microscopy (FESEM), and EDS investigations provide an in-depth analysis of the structural, morphological, and compositional characteristics of Ti<sub>3</sub>C<sub>2</sub>-BiVO<sub>4</sub> sheets. The XRD analysis proves the successful combination of different materials and the presence of crystalline phases. The FESEM imaging technique exposes the shape and arrangement of particles in sheets, while the EDS analysis verifies the elemental composition and uniform distribution. These investigations show that Ti<sub>3</sub>C<sub>2</sub>-BiVO<sub>4</sub> composites have been successfully synthesized, indicating their potential for use in anti-cancer applications.

#### How to cite this article

Lakshmi Anvitha N, A G, S V, et al. (June 01, 2024) Facile Fabrication of Titanium Carbide (Ti<sub>3</sub>C<sub>2</sub>)-Bismuth Vanadate (BiVO<sub>4</sub>) Nano-Coupled Oxides for Anti-cancer Activity. Cureus 16(6): e61492. DOI 10.7759/cureus.61492

**Categories:** Dentistry, Radiation Oncology, Oncology

**Keywords:** nano-coupled oxides, anti-cancer activity, energy dispersive spectrum, bismuth vanadate,  $\text{Ti}_3\text{C}_2$

## Introduction

Cancer has a significant and extensive influence on human existence, impacting people, families, and society globally. Cancer is a leading cause of illness and death worldwide, with millions of new cases detected each year and millions of lives lost to the disease. Cancer may induce physical discomfort, exhaustion, and a range of other symptoms that vary based on the specific kind and stage of the illness [1]. Medical interventions such as chemotherapy, radiation treatment, and surgery may exert a considerable toll on the body and can result in substantial adverse reactions. Cancer may also lead to pain and discomfort, fatigue, cachexia, immune system suppression, and cognitive impairment that have an impact on the overall well-being and satisfaction of people [2]. Nevertheless, these obstacles in the fields of cancer research, prevention, early diagnosis, and therapy have resulted in enhancements in the rates of survival and the overall well-being of several individuals afflicted with cancer. Nevertheless, there is still a significant amount of work that has to be accomplished to tackle the worldwide impact of cancer and guarantee the fair and equal availability of cancer treatment for every person [3].

In 2024, the worldwide cancer burden will continue to be substantial. The World Health Organization (WHO) reported that there were an estimated 20 million new cancer diagnoses and 9.7 million deaths attributable to cancer in 2022. Approximately 53.5 million individuals worldwide were predicted to be living with cancer within five years after being diagnosed. Although surgery, chemotherapy, and radiotherapy are widely considered to be the most popular cancer treatment options, they are not always effective. Chemotherapy and radiotherapy, while very effective, have serious adverse effects when used [4]. The progressive resistance of cancer cells to treatment is one of the major issues with cancer treatment. The emergence of cancer cell lines resistant to chemotherapeutic drugs is a time-tested method for examining the causes of cytotoxicity and drug resistance in chemotherapeutic drugs. The quantity of healthy cells in a sample is known as cell viability, and the growth of cells is a key sign for comprehending the processes underlying the actions of certain genes, proteins, and pathways involved in a cell's ability to survive or die after being exposed to harmful substances. Chemotherapeutics' non-selective therapeutic strategy fundamentally makes it impossible to efficiently eradicate cancer stem cells (CSCs) [5].

If a chemotherapeutic agent is employed in combination therapy, the toxicity is greatly reduced because alternative routes will be targeted. In the end, this has a synergistic or cumulative effect, necessitating a lower therapeutic dosage of each medicine alone. Titanium carbide ( $\text{Ti}_3\text{C}_2$ ) belongs to the group of two-dimensional materials called MXene. Although research on the anti-cancer properties of  $\text{Ti}_3\text{C}_2$  is still in its nascent phase, several studies have shown its promising potential in this domain [6]. One suggested mechanism for the anti-cancer action of  $\text{Ti}_3\text{C}_2$  is its capacity to trigger cancer cell apoptosis via many routes.  $\text{Ti}_3\text{C}_2$  has shown cytotoxic properties against cancer cells by inducing apoptosis, a process of programmed cell death. In addition,  $\text{Ti}_3\text{C}_2$  has the ability to trigger autophagy, which is a cellular mechanism that results in the breakdown and reuse of damaged or unneeded cellular parts, therefore promoting the death of cancer cells. Moreover, much research has been conducted on  $\text{Ti}_3\text{C}_2$  nanoparticles to explore their potential as carriers for delivering drugs in the field of cancer treatment [7].

$\text{Ti}_3\text{C}_2$  nanoparticles possess distinctive physicochemical characteristics, such as a substantial surface area and functional groups, which enable them to effectively encapsulate and transport anti-cancer medicines to specific tumor locations. This strategy of tailored medication delivery decreases the negative effects on unintended areas and improves the effectiveness of anti-cancer treatments while decreasing their overall toxicity in the body. Furthermore,  $\text{Ti}_3\text{C}_2$ -based nanomaterials have been investigated for their capacities in photothermal therapy (PTT).  $\text{Ti}_3\text{C}_2$  nanoparticles, when subjected to near-infrared (NIR) light, have the ability to produce heat, resulting in localized hyperthermia specifically inside tumors [8]. Hyperthermia caused by this method leads to the killing of cancer cells while preserving nearby healthy tissues, making PTT a very promising strategy for treating cancer.  $\text{Ti}_3\text{C}_2$  has promise in its ability to combat cancer via many methods, such as direct cytotoxicity, medication delivery, and PTT. Bismuth vanadate ( $\text{BiVO}_4$ ) is an n-type semiconductor made up of elements that are comparatively common on Earth. Its advantages have led to its widespread use as a photoanode for photoelectrochemical (PEC) water splitting. It possesses a direct bandgap of 2.4 eV in the monoclinic phase, with a conduction band position near to 0 V vs. normal hydrogen electrode (NHE) (pH = 0) and a valence band position at +2.4 eV vs. NHE (pH = 0) [9].  $\text{BiVO}_4$  is an adaptable material that has great potential for use in biomedical fields such as wound healing, photodynamic therapy, biosensing, and antibacterial treatment. Due to its unique characteristics, it is a promising material for future studies in photocatalysis and biocompatibility. Additional medical uses for  $\text{BiVO}_4$ , including novel approaches to illness prevention and treatment, are anticipated as a result of ongoing developments in nanotechnology and materials science [10].

The high efficiency of bismuth (Bi) in treating pathogens, viruses, and cancerous tumors is a major factor in its use in medicine and healthcare. Compounds containing Bi have been widely shown to offer potential

anti-cancer effects on malignant tumor cell lines. Bi (III) compounds' anti-cancer mechanism is primarily linked to the production of reactive oxygen species (ROS), a decrease in mitochondrial membrane potential, and the triggering of apoptosis. Bi-based anti-cancer drugs' precise mode of action, however, is still unknown [11]. Future research on Bi compounds as anti-cancer agents at the mechanistic and therapeutic levels may provide a new avenue. Although Bi is thought to be harmless, as previously indicated, prolonged exposure to it may have some adverse effects on human subjects.  $\text{BiVO}_4$  is a promising material because of its properties of visible light absorption, great chemical stability, non-toxicity, and low cost. We are going to synthesize  $\text{Ti}_3\text{C}_2$  modified by  $\text{BiVO}_4$ , and it will be characterized by different analytical methodologies. Optimized materials are used for anti-cancer activity in cancer cell lines.  $\text{Ti}_3\text{C}_2$  electrochemical energy storage is ensured by its 2D form, excellent electrical characteristics, and biocompatibility [12].

The features of visible light absorption, strong chemical stability, non-toxicity, and inexpensive cost make  $\text{BiVO}_4$  a promising material. MXene is used in surface-enhanced Raman spectroscopy (SERS) to detect extremely small amounts of anti-cancer medicine. Favorable biocompatibility and ideal mechanical properties make them expand their application in the cancer therapy field. A material called MXene epigallocatechin gallate (EGCG) complex nanosheets may improve cancer PTT, and it has anti-inflammatory properties [13]. It was suggested that clinical cancer therapy and treatment are greatly aided by the quick, reliable detection of carcinogenic embryonic antigen, and it demonstrates that they have good bactericidal action, accelerating the healing of postoperative wounds without losing their ability to prevent recurrence. The current investigation comprised the preparation of  $\text{Ti}_3\text{C}_2$ - $\text{BiVO}_4$  heterostructures utilizing a modified synthesis process that involved hydrofluoric acid (HF) etching followed by a hydrothermal technique [14]. The  $\text{Ti}_3\text{C}_2$ - $\text{BiVO}_4$  nanosheets have been prepared and have exceptional behavior in both synthetic procedures and characterization studies. The presence of  $\text{Ti}_3\text{C}_2$ - $\text{BiVO}_4$  nanomaterials was verified using X-ray diffraction (XRD), scanning electron microscopy (SEM), and energy-dispersive spectroscopy (EDS) investigation, which included examining their crystalline behavior, phase, surface morphology, and elemental composition. The study examined the anti-cancer characteristics of  $\text{Ti}_3\text{C}_2$ - $\text{BiVO}_4$  that was artificially produced. A cell viability study was conducted in vitro on colorectal cancer (CRC) cell lines to assess the biocompatibility of  $\text{Ti}_3\text{C}_2$ - $\text{BiVO}_4$ .

## Materials And Methods

The preparation of  $\text{Ti}_3\text{C}_2$  using HF is to etch the layers of aluminum (Al) from titanium aluminum carbide ( $\text{Ti}_3\text{AlC}_2$ ) (MAX phases), where "M" stands for a transition metal (titanium (Ti)) and "A" for an element (Al). To prepare the 2D  $\text{Ti}_3\text{C}_2$  MXene, 2.5 g of  $\text{Ti}_3\text{AlC}_2$  powder was dissolved in 60 mL of a 40% HF solution in a polytetrafluoroethylene (PTFE) container. The etching process was made more efficient and completed in 24 hours by using a magnetic stirring system to keep the mixture stirred and heated continuously. The centrifugation was performed at 4000 rpm for five minutes. Subsequently, deionized water was used to wash the solution many times until its pH reached around 7. The appropriate  $\text{Ti}_3\text{C}_2$  powder was made by vacuum drying the acquired sediment at 80°C for 24 hours.

Monoclinic  $\text{BiVO}_4$  materials were synthesized via a hydrothermal method. Typically, 10 mmol of bismuth nitrate ( $\text{Bi}(\text{NO}_3)_3 \cdot 5\text{H}_2\text{O}$ ) was dissolved in 100 mL of a 2 mol/L  $\text{HNO}_3$  solution and stirred uniformly. Subsequently, 10 mmol of ammonium metavanadate ( $\text{NH}_4\text{VO}_3$ ) was added to the mixed solution. After being stirred for one hour, the mixture was transferred into a 100 mL sealed Teflon-lined stainless steel autoclave at 180°C for 16 hours. After cooling to room temperature, the precipitate was washed three times with deionized water, ethanol, and acetone, respectively (solution A). Finally, the precipitate was dried at 80°C, followed by calcination at 450°C for three hours to obtain  $\text{BiVO}_4$ .

The prepared  $\text{Ti}_3\text{C}_2$  was dispersed in 20 mL of dimethyl sulfoxide (DMSO) and sonicated for three hours (solution B). Then the solution B was dropwise added to the solution A and stirred for two hours at 90°C. The reaction mixture is transferred to a hydrothermal process at 180°C for 12 hours. After cooling to room temperature, the precipitate was washed three times with deionized water, ethanol, and acetone. After preparation, the materials are characterized using XRD, SEM, and EDS analysis. The XRD study allows us to explain the crystalline behavior and phase purity of the material. SEM images are utilized to examine the surface morphology and evaluate the average particle size, as well as to determine the pressure exerted on the surface. EDS analysis confirmed the elements' composition.

The 3-(4,5-dimethylthiazol-2-yl)-2,5-diphenyltetrazolium bromide (MTT) test is often used to check for cell viability and proliferation. It uses colorimetric assays to measure how metabolically active cells change a yellow tetrazolium salt called MTT into formazan crystals. The CRC cells (HCT116) are evenly distributed over the wells of a multi-well plate and left to adhere for the night. Different concentrations of  $\text{Ti}_3\text{C}_2$ - $\text{BiVO}_4$  nanosheets are used to treat cells, usually ranging from very low to very high. To compare the results, we also include control groups of cells that were either not treated or treated with vehicle control, such as culture media. It is common practice to incubate cells with nanosheets for a certain amount of time after treatment, usually 48 hours, so that the nanosheets can exert their cytotoxic effects. The MTT reagent is

added to each well after the incubation time, and the cells are incubated for an additional duration, typically 2-4 hours. Purple formazan crystals are formed when metabolically active cells decrease the MTT reagent. An aspiration of the culture media containing the MTT reagent is performed after incubation. A solvent, such as DMSO, is then added to dissolve the formazan crystals, producing a solution that is purple in color. Using a microplate reader, the absorbance of the purple formazan solution is measured spectrophotometrically at a wavelength usually about 570 nm. Optimal cell density in a culture is a good indicator of absorbance intensity. We can determine the relative percentages of cell viability or cytotoxicity from the MTT absorbance readings compared to the control groups. In order to find the concentration of  $\text{Ti}_3\text{C}_2\text{-BiVO}_4$  nanosheets that inhibits cell viability by half, a dose-response curve is constructed, and the IC50 value is calculated.

## Results

### XRD analysis

XRD analysis determined the crystalline behavior of the prepared  $\text{Ti}_3\text{C}_2\text{-BiVO}_4$  materials. Figure 1 shows that the most prominent diffraction peak for the (104) plane of  $\text{Ti}_3\text{AlC}_2$ ,  $2\theta$  at  $39.0^\circ$ , disappeared after HF treatment, suggesting the elimination of the Al layers of MAX phase  $\text{Ti}_3\text{AlC}_2$  [15]. The diffraction peaks at  $19.1^\circ$ , corresponding to the (004) plane, exhibited a downward shift in their angles and increased broadness. This phenomenon was attributed to an expansion in the distance between layers of  $\text{Ti}_3\text{C}_2$  [16].

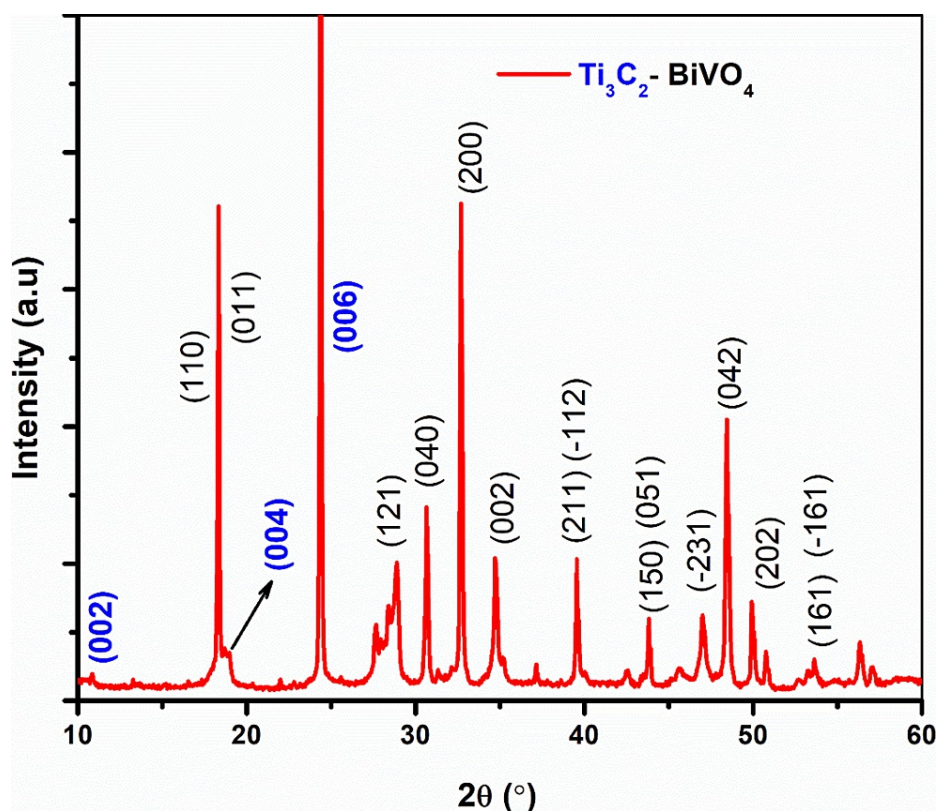


**FIGURE 1: XRD pattern of  $\text{Ti}_3\text{C}_2\text{-BiVO}_4$**

XRD: X-ray diffraction;  $\text{BiVO}_4$ : bismuth vanadate;  $\text{Ti}_3\text{C}_2\text{-BiVO}_4$ : titanium carbide (MXene)-bismuth vanadate

The peaks associated with  $\text{BiVO}_4$  were seen at  $2\theta = 18.3^\circ, 18.5^\circ, 28.79^\circ, 31.7^\circ, 32.6^\circ, 34.48^\circ, 36.19^\circ, 40.1^\circ, 43.54^\circ, 47.1^\circ, 48.6^\circ, 50.6^\circ, 55.4^\circ, \text{ and } 58.85^\circ$ , which correspond to the (110), (011), (121), (040), (200), (002), (211), (-112), (150), (051), (-231), (042), (202), (161), and (-161) diffraction planes, respectively. The diffraction pattern is in good agreement with Joint Committee on Powder Diffraction Standards (JCPDS) card no. 14-0688, which confirms the presence of the monoclinic phase of  $\text{BiVO}_4$ . The sharp peaks indicate the high crystalline nature of  $\text{Ti}_3\text{C}_2\text{-BiVO}_4$ . The intense and distinct peak patterns closely correspond to a monoclinic phase of  $\text{BiVO}_4$ . The diffraction planes of (002), (004), and (006) confirm the formation of  $\text{Ti}_3\text{C}_2$ . No other impurities are present in the  $\text{Ti}_3\text{C}_2\text{-BiVO}_4$  materials (Figure 1).

### EDS analysis

EDS analysis identifies and quantifies the elements present in the  $\text{Ti}_3\text{C}_2\text{-BiVO}_4$  sample. The primary constituents of  $\text{Ti}_3\text{C}_2$  are Ti and carbon (C). The EDS spectrum displays characteristic X-ray peaks corresponding to these elements. In this spectrum, Ti was found to be 23.51%, C 19.94%, oxygen (O) 42.25%, Bi 11.9%, and vanadium (V) 2.04%. All these compounds are depicted in the below EDS analysis. This confirms the presence of only the elements of the compound, indicating no impurities were observed (Figure 2).

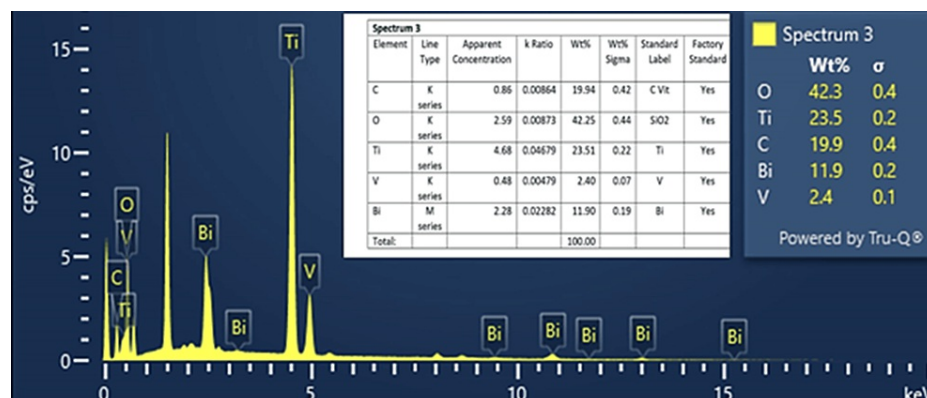


**FIGURE 2: EDS analysis of  $\text{Ti}_3\text{C}_2$  and  $\text{BiVO}_4$**

EDS: energy-dispersive spectroscopy,  $\text{Ti}_3\text{C}_2$ : titanium carbide;  $\text{BiVO}_4$ : bismuth vanadate; O: oxygen; Ti: titanium; C: carbon; Bi: bismuth; V: vanadium

## SEM analysis

$\text{Ti}_3\text{C}_2\text{-BiVO}_4$  materials typically exhibit a sheet-like structure with a large lateral size. SEM images can capture the presence of interconnected networks of nanosheets, providing insights into the exfoliation and delamination processes during  $\text{Ti}_3\text{C}_2\text{-MXene}$  synthesis. It was analyzed and found to be 0.5 micrometers thick. Many voids and gaps were observed in the sheets.  $\text{BiVO}_4$  particles can be seen on and between the  $\text{Ti}_3\text{C}_2$  sheets. The SEM images of  $\text{Ti}_3\text{C}_2\text{-BiVO}_4$  composites reveal a sheet-like structure that is composed of interconnecting layers or flakes with varied thicknesses. The  $\text{Ti}_3\text{C}_2$  layers are a framework on which  $\text{BiVO}_4$  nanoparticles or nanosheets are attached. This configuration has several benefits for anti-cancer purposes. The sheet-like morphology of  $\text{Ti}_3\text{C}_2\text{-BiVO}_4$  composites offers a large surface area, which is advantageous for enhancing the quantity of active sites accessible for anti-cancer applications. The combination of  $\text{Ti}_3\text{C}_2$  and  $\text{BiVO}_4$  may lead to synergistic effects, where the distinct features of each component complement and increase the total efficiency (Figure 3).



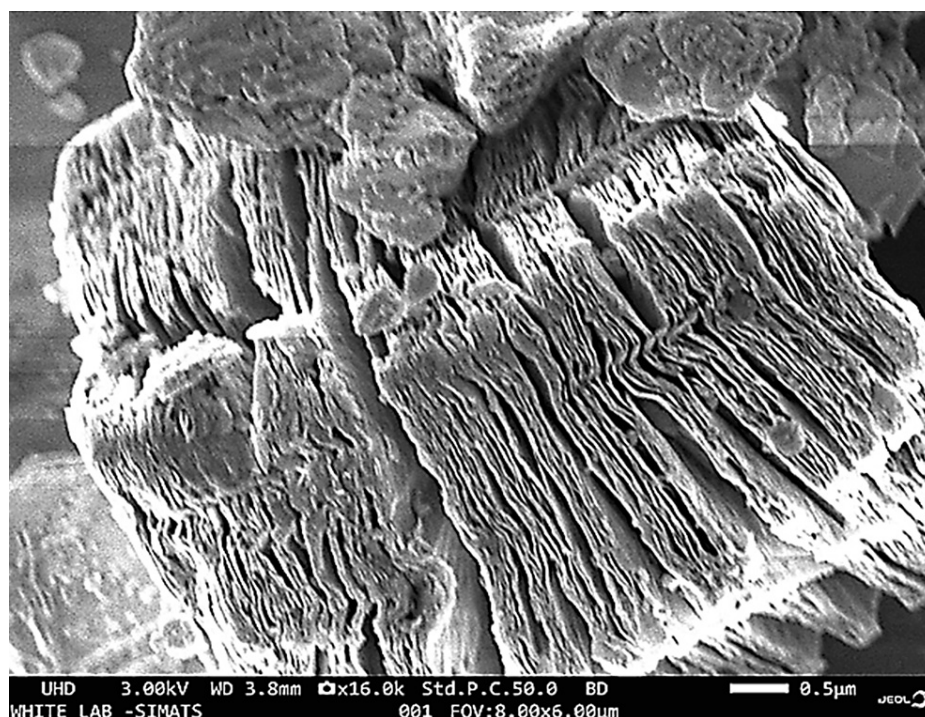


**FIGURE 3: SEM images of the Ti<sub>3</sub>C<sub>2</sub>-BiVO<sub>4</sub>**

SEM: scanning electron microscopy; Ti<sub>3</sub>C<sub>2</sub>-BiVO<sub>4</sub>: titanium carbide (MXene)-bismuth vanadate

## Anti-cancer activity

It depicts cell death, demonstrating that this compound exhibits good anti-cancer activity when detected with the MTT assay using colon cancer cells (Figure 4). The unique physicochemical features and capacity to selectively target cancer cells of nanomaterials, including Ti<sub>3</sub>C<sub>2</sub>-BiVO<sub>4</sub> nanosheets, have made them a viable method for cancer treatment. In this article, we go into the specifics of how Ti<sub>3</sub>C<sub>2</sub>-BiVO<sub>4</sub> nanosheets fight CRC cells. The photocatalytic characteristics of Ti<sub>3</sub>C<sub>2</sub>-BiVO<sub>4</sub> nanosheets allow them to produce ROS when exposed to light. DNA damage, lipid peroxidation, and protein oxidation are outcomes of ROS induction in cancer cells, which includes singlet oxygen ( $^1\text{O}_2$ ) and superoxide radicals ( $\text{O}_2^-$ ). Cancer cells undergo apoptotic cell death when this oxidative stress upsets their balance. Cancer cells are able to absorb Ti<sub>3</sub>C<sub>2</sub>-BiVO<sub>4</sub> nanosheets because of their small size and distinctive physicochemical characteristics. Nanosheets have anti-cancer properties when they are absorbed and localized to the cytoplasm and nucleus. To ensure the effective delivery of therapeutic payloads to target CRC cells, the addition of BiVO<sub>4</sub> increases the nanosheets' biocompatibility and stability. By causing mitochondrial membrane depolarization, reducing adenosine triphosphate (ATP) generation, and increasing cytochrome c release into the cytoplasm, Ti<sub>3</sub>C<sub>2</sub>-BiVO<sub>4</sub> nanosheets interfere with mitochondrial activity in CRC cells. Cell death, DNA breakage, and caspase activation are the outcomes of these processes, which trigger the intrinsic apoptotic pathway. G<sub>0</sub>/G<sub>1</sub> or G<sub>2</sub>/M cell cycle arrest is induced in CRC cells by treatment with Ti<sub>3</sub>C<sub>2</sub>-BiVO<sub>4</sub> nanosheets. Cell cycle inhibitors like p21 and p27 are upregulated, whereas cyclins and cyclin-dependent kinases (CDKs) are downregulated, mediating this arrest. Consequently, CRC cells are rendered incapable of undergoing cell cycle progression and apoptotic cell death. Key signaling pathways involved in the advancement of CRC, such as the PI3K/AKT/mTOR, MAPK/ERK, and Wnt/ $\beta$ -catenin pathways, are modulated by Ti<sub>3</sub>C<sub>2</sub>-BiVO<sub>4</sub> nanosheets. The nanosheets have strong anti-cancer properties by reducing CRC cell motility, invasion, and survival via blocking the activation of these pathways. Ti<sub>3</sub>C<sub>2</sub>-BiVO<sub>4</sub> nanosheets improve the immune response to cancer in CRC, demonstrating immunomodulatory characteristics. The immune system is able to identify and eliminate CRC cells because the nanosheets activate and infiltrate cytotoxic T lymphocytes (CTLs), natural killer (NK) cells, and dendritic cells (DCs) into the tumor microenvironment. Against CRC cells, Ti<sub>3</sub>C<sub>2</sub>-BiVO<sub>4</sub> nanosheets induce ROS-mediated oxidative stress, alter mitochondrial function, stop the cell cycle, block signaling pathways, and modulate the immunological response, among other multi-faceted anti-cancer activities. These results emphasize the promise of Ti<sub>3</sub>C<sub>2</sub>-BiVO<sub>4</sub> nanosheets as an innovative approach to treating CRC.

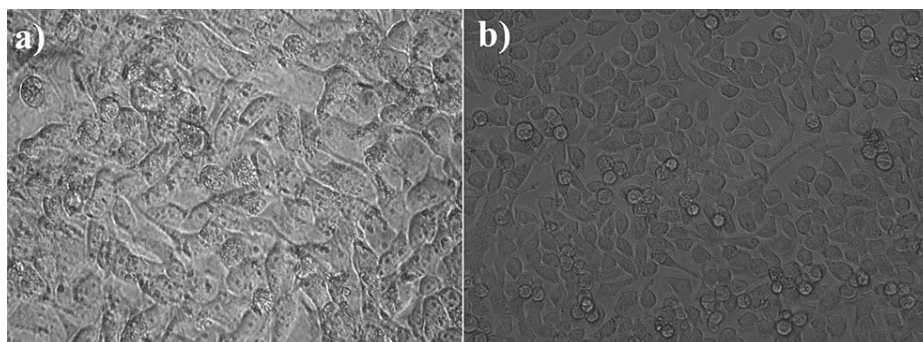


**FIGURE 4: Anti-cancer activity of the  $\text{Ti}_3\text{C}_2\text{-BiVO}_4$  (a) control and (b) after 48 hours**

$\text{BiVO}_4$ : bismuth vanadate;  $\text{Ti}_3\text{C}_2\text{-BiVO}_4$ : titanium carbide (MXene)-bismuth vanadate

## Discussion

Jastrzębska et al. analyzed the cancer applications of MXene and found that MXene has great anti-cancer potential and promising in vitro and in vivo results, which help in the precise drug delivery of MXene [17]. Badrigilan et al. analyzed the role of MXene in breast cancer and found that it reduced cytotoxicity and showed a great surface-to-volume ratio [18]. Zhang et al. analyzed the anti-cancer properties of MXene which showed that MXene kills human cancer cells by using certain mechanisms [19]. Jastrzębska et al. analyzed the cytotoxicity of delaminated MXene and obtained that MXene used the oxidative stress method to kill the cancerous cells present and reduce the cytotoxicity to an extent [17]. Jolly et al. reviewed the advances in cancer treatment using Bi-based nanoparticles and captured that, due to their low toxicity, X-ray sensitivity, high atomic number, near-infrared-driven semiconductor qualities, and low cost, multifunctional nanomaterials based on Bi have significant potential for the treatment and diagnostics of cancer [20]. Here, a thorough analysis of recent developments in the medical uses of Bi-based nanomaterials is presented, covering such topics as assessments of in-tumor site accumulation, tumor targeting, and therapeutic performance, as well as the features, advantages, and drawbacks of major monotherapies mediated by Bi-based nanomaterial. Badrigilan et al. reported that an efficient theranostic for clinical cancer treatment can be obtained by combining high-performance CT imaging and PTT into one nanoprobe [18]. Such nanotheranostics have acceptable blood compatibility, cytotoxicity, and physiological dispersity. Bi nanoparticles have a strong and constant absorbance profile in the NIR region, high photostability, and remarkable photothermal efficiency of 30.0%. The outcomes show graphene quantum dots (GQDs)-Bi nanoparticles' promise as a successful therapeutic nanoagent for CT imaging and cancer PTT [21]. Shumin after analyzing reported that due to their favorable characteristics, including low toxicity, excellent X-ray absorption, and ease of fabrication, Bi-based nanoparticles are extensively researched in the detection and therapy of cancer. However, due to poor tumor site targeting, lengthy retention-induced systemic toxicity, and immune resistance, pure Bi alone cannot produce both effective and safe radiotherapy results. When paired with various therapies like PTT and high-intensity focused ultrasound (HIFU), bio-based nanoparticles show synergistic anti-cancer potential. Zhang reported regarding XRD that the peaks of high-purity  $\text{Ti}_3\text{AlC}_2$  powders can be seen with only a small amount of TiC and the XRD patterns reflect the level of Al etching. After 40 hours of HF reaction, the peak at  $239^\circ$  that corresponds to  $\text{Ti}_3\text{AlC}_2$ 's distinctive peak (104) completely vanished, indicating that Al has been removed from the compound. Parallel to this, the (002) diffraction peaks at  $29.5^\circ$  [22]. Jolly et al. reported that the XRD pattern showed that  $\text{Al}_2\text{O}_3$ , TiC, and  $\text{Ti}_3\text{AlC}_2$  were present. Following the trend shown by earlier work producing  $\text{Ti}_3\text{AlC}_2$  and  $\text{Ti}_2\text{AlC}$  from  $\text{TiO}_2$ , the XRD patterns from the 3.0:5.5:1.9 and 3.0:6.0:2.0 ratios and the previously mentioned temperature changes showed more  $\text{Al}_2\text{O}_3$  and TiC relative to  $\text{Ti}_3\text{AlC}_2$  [20]. Evident from the lower intensity of the TiC diffraction peaks (around  $2\theta$  of  $36.0^\circ$ ,  $41.9^\circ$ ,  $60.7^\circ$ , and  $72.6^\circ$ ) compared to those detected for the 3.0:5.5:1.9 ratio, a lower content of TiC was achieved for 3.0:6.0:1.9 [23].

## Limitation

Enhancing the yield, repeatability, and scalability of the fabrication process through the optimization of the synthesis method; improving the stability, biocompatibility, and targeting abilities of  $\text{Ti}_3\text{C}_2\text{-BiVO}_4$  nanomaterial-linked oxides by investigating surface modification strategies; and exploring potential synergies by integrating  $\text{Ti}_3\text{C}_2\text{-BiVO}_4$  nanomaterials with other therapeutic methods like radiation therapy, immunotherapy, or chemotherapy are the efforts that could contribute to the development of more effective and versatile cancer treatment strategies in the future.

## Conclusions

The investigation demonstrated the simple synthesis of  $\text{Ti}_3\text{C}_2\text{-BiVO}_4$  and their potential for use in cancer treatment. A composite material with improved anti-cancer capabilities was produced by integrating  $\text{Ti}_3\text{C}_2$  MXenes with  $\text{BiVO}_4$  using an efficient and easy synthesis technique. The fabrication of the  $\text{Ti}_3\text{C}_2\text{-BiVO}_4$  composite was confirmed by the XRD study. The final product was determined to include both  $\text{Ti}_3\text{C}_2$  and  $\text{BiVO}_4$  because characteristic peaks corresponding to both components were detected. In addition to confirming the high purity of  $\text{Ti}_3\text{C}_2\text{-BiVO}_4$  materials, the XRD patterns showed no obvious impurities. The long-term performance of the composite under evaluation circumstances was suggested by the well-maintained crystalline structure and phase composition. Using SEM, the morphology and structural properties of the  $\text{Ti}_3\text{C}_2\text{-BiVO}_4$  were thoroughly examined. The SEM images showed that the  $\text{Ti}_3\text{C}_2$  sheets had a uniform distribution of  $\text{BiVO}_4$  nanoparticles, creating a composite that was well-dispersed. By increasing the surface area and offering active sites, the morphology study showed that the  $\text{BiVO}_4$  nanoparticles were evenly anchored on the  $\text{Ti}_3\text{C}_2$  surface. In order to enhance the material's interaction with cancer cells during photodynamic treatment, this morphological trait is essential. The  $\text{Ti}_3\text{C}_2\text{-BiVO}_4$  composite's elemental composition was validated using EDS studies. By displaying clear peaks for Ti, C, Bi, V, and O in the EDS spectra, the  $\text{Ti}_3\text{C}_2$  matrix was shown to have successfully incorporated  $\text{BiVO}_4$ . The composite caused cancer cells to undergo oxidative stress and cell death by producing ROS.  $\text{Ti}_3\text{C}_2$  and  $\text{BiVO}_4$  worked together to increase the composite's photodynamic treatment efficacy by boosting ROS generation efficiency. This composite shows promise for clinical use in cancer therapy due to its biocompatibility and low toxicity to healthy cells.

## Additional Information

### Author Contributions

All authors have reviewed the final version to be published and agreed to be accountable for all aspects of the work.

**Concept and design:** Ilangovar I.G.K, Nagubandi Lakshmi Anvitha, Geetha A, Vasugi S, Balachandran S

**Acquisition, analysis, or interpretation of data:** Ilangovar I.G.K, Nagubandi Lakshmi Anvitha, Geetha A, Vasugi S, Balachandran S

**Drafting of the manuscript:** Ilangovar I.G.K, Nagubandi Lakshmi Anvitha, Geetha A, Vasugi S, Balachandran S

**Critical review of the manuscript for important intellectual content:** Ilangovar I.G.K, Nagubandi Lakshmi Anvitha, Geetha A, Vasugi S, Balachandran S

**Supervision:** Ilangovar I.G.K, Balachandran S

### Disclosures

**Human subjects:** All authors have confirmed that this study did not involve human participants or tissue.

**Animal subjects:** All authors have confirmed that this study did not involve animal subjects or tissue.

**Conflicts of interest:** In compliance with the ICMJE uniform disclosure form, all authors declare the following: **Payment/services info:** All authors have declared that no financial support was received from any organization for the submitted work. **Financial relationships:** All authors have declared that they have no financial relationships at present or within the previous three years with any organizations that might have an interest in the submitted work. **Other relationships:** All authors have declared that there are no other relationships or activities that could appear to have influenced the submitted work.

### Acknowledgements

The authors would like to express their gratitude to the Department of Physiology, Saveetha Dental College and Hospitals, Saveetha Institute of Medical and Technical Sciences, Saveetha University, Chennai 600077, Tamil Nadu, India, for providing infrastructure facilities and funding support for this study.

## References

1. Siegel RL, Miller KD, Jemal A: Cancer statistics, 2020. *CA Cancer J Clin.* 2020, 70:7-30. [10.3322/caac.21590](#)
2. Padmapriya A, Preetha S, Selvaraj J, Sridevi G: Effect of Carica papaya seed extract on IL -6 and TNF- $\alpha$  in human lung cancer cell lines - an In vitro study. *Res J Pharm Technol.* 2022, 10:5478-82.
3. Rifaath M, Santhakumar P, Selvaraj J: Effect of Carica papaya on beta catenin and Wnt mRNA expression in human colon cancer (HT-29) cells in vitro. *Bioinformation.* 2022, 18:289-92.
4. Devabattula G, Panda B, Yadav R, Godugu C: The potential pharmacological effects of natural product withaferin A in cancer: opportunities and challenges for clinical translation. *Planta Med.* 2024, 90:440-53. [10.1055/a-2289-9600](#)
5. Tabish TA, Hamblin MR: Mitochondria-targeted nanoparticles (mitoNANO): an emerging therapeutic



- shortcut for cancer. *Biomater Biosyst*. 2021, 3:100023. [10.1016/j.bbiosy.2021.100023](https://doi.org/10.1016/j.bbiosy.2021.100023)
6. Sadiq M, Pang L, Johnson M, Sathish V, Zhang Q, Wang D: 2D nanomaterial, Ti3C2 MXene-based sensor to guide lung cancer therapy and management. *Biosensors (Basel)*. 2021, 11:40. [10.3390/bios11020040](https://doi.org/10.3390/bios11020040)
7. Ranjbari S, Darroudi M, Hatamluyi B, Arefinia R, Aghaee-Bakhtiari SH, Rezayi M, Khazaei M: Application of MXene in the diagnosis and treatment of breast cancer: a critical overview. *Front Bioeng Biotechnol*. 2022, 10:984336. [10.3389/fbioe.2022.984336](https://doi.org/10.3389/fbioe.2022.984336)
8. Darroudi M, Elnaz Nazari S, Karimzadeh M, et al.: Two-dimensional-Ti3C2 magnetic nanocomposite for targeted cancer chemotherapy. *Front Bioeng Biotechnol*. 2023, 11:1097631. [10.3389/fbioe.2023.1097631](https://doi.org/10.3389/fbioe.2023.1097631)
9. Kim SJ, Kim HS, Seo YR: Understanding of ROS-inducing strategy in anticancer therapy. *Oxid Med Cell Longev*. 2019, 2019:5381692. [10.1155/2019/5381692](https://doi.org/10.1155/2019/5381692)
10. Prasad MD, Ramesh GV, Batabyal SK: 2D layered structure of bismuth oxyhalides for advanced applications. *ACS Symposium Series*. American Chemical Society, Washington, DC; 2020. 1353:295-315. [10.1021/bk-2020-1353.ch012](https://doi.org/10.1021/bk-2020-1353.ch012)
11. Liu P, Yi J, Bao R, Zhao H: Theory-oriented synthesis of 2D/2D BiVO4/MXene heterojunction for simultaneous removal of hexavalent chromium and methylene blue. *ChemCatChem*. 2021, 13:3046-53. [10.1002/cctc.202100315](https://doi.org/10.1002/cctc.202100315)
12. Liao T, Chen Z, Kuang Y, et al.: Small-size Ti3C2Tx MXene nanosheets coated with metal-polyphenol nanodots for enhanced cancer photothermal therapy and anti-inflammation. *Acta Biomater*. 2023, 159:312-23. [10.1016/j.actbio.2023.01.049](https://doi.org/10.1016/j.actbio.2023.01.049)
13. Venkatesan R, Velumani S, Ordon K, Makowska-Janusik M, Corbel G, Kassiba A: Nanostructured bismuth vanadate (BiVO4) thin films for efficient visible light photocatalysis. *Mater Chem Phys*. 2018, 205:325-33. [10.1016/j.matchemphys.2017.11.004](https://doi.org/10.1016/j.matchemphys.2017.11.004)
14. Zhang RX, Wong HL, Xue HY, Eoh JY, Wu XY: Nanomedicine of synergistic drug combinations for cancer therapy - strategies and perspectives. *J Control Release*. 2016, 240:489-503. [10.1016/j.jconrel.2016.06.012](https://doi.org/10.1016/j.jconrel.2016.06.012)
15. Kumar ET, Thirumalai K, Balachandran S, Aravindhan R, Swaminathan M, Raghava Rao J: Solar light driven degradation of post tanning water at heterostructured BiVO4-ZnO mixed oxide catalyst interface. *Surf Interfaces*. 2017, 8:147-53. [10.1016/j.surf.2017.05.009](https://doi.org/10.1016/j.surf.2017.05.009)
16. Cao S, Shen B, Tong T, Fu J, Yu J: 2D/2D heterojunction of ultrathin MXene/Bi2WO6 nanosheets for improved photocatalytic CO2 reduction. *Adv Funct Mater*. 2018, 28:1800136. [10.1002/adfm.201800136](https://doi.org/10.1002/adfm.201800136)
17. Jastrzębska AM, Szuplewska A, Wojciechowski T, et al.: In vitro studies on cytotoxicity of delaminated Ti3C2 MXene. *J Hazard Mater*. 2017, 339:1-8. [10.1016/j.jhazmat.2017.06.004](https://doi.org/10.1016/j.jhazmat.2017.06.004)
18. Badrigilan S, Shaabani B, Aghaji NG, Mesbahi A: Graphene quantum dots-coated bismuth nanoparticles for improved CT imaging and photothermal performance. *Int J Nanosci*. 2020, 19:1850043. [10.1142/S0219581X18500436](https://doi.org/10.1142/S0219581X18500436)
19. Zhang Y, Yan Y, Qiu H, Ma Z, Ruan K, Gu J: A mini-review of MXene porous films: preparation, mechanism and application. *J Mater Sci Technol*. 2022, 103:42-9. [10.1016/j.jmst.2021.08.001](https://doi.org/10.1016/j.jmst.2021.08.001)
20. Jolly S, Paranthaman MP, Naguib M: Synthesis of Ti3C2Tx MXene from low-cost and environmentally friendly precursors. *Mater Today Adv*. 2021, 10:100139. [10.1016/j.mtaadv.2021.100139](https://doi.org/10.1016/j.mtaadv.2021.100139)
21. Hong C, Chen T, Wu M, et al.: Bismuth-based two-dimensional nanomaterials for cancer diagnosis and treatment. *J Mater Chem B*. 2023, 11:8866-82. [10.1039/d3tb01544k](https://doi.org/10.1039/d3tb01544k)
22. Zhang L, Alimu G, Du Z, et al.: Functionalized magnetic nanoparticles for NIR-induced photothermal therapy of potential application in cervical cancer. *ACS Omega*. 2023, 8:21793-801. [10.1021/acsomega.3c01374](https://doi.org/10.1021/acsomega.3c01374)
23. Su T, Hood ZD, Naguib M, et al.: 2D/2D heterojunction of Ti3C2/g-C3N4 nanosheets for enhanced photocatalytic hydrogen evolution. *Nanoscale*. 2019, 11:8138-49. [10.1039/c9nr00168a](https://doi.org/10.1039/c9nr00168a)